

Improved IMU-based Human Activity Recognition using Hierarchical HMM Dissimilarity

Sara Ashry^{1,2}, Walid Gomaa^{1,3}, Mubarak G. Abdu-Aguye⁴ and Nahla El-borae¹

¹*Cyber-Physical Systems Lab (CPS), Computer Science and Engineering Department (CSE), Egypt-Japan University of Science and Technology (E-JUST), Alexandria, Egypt*

²*Computers and Systems Department, Electronic Research Institute (ERI), Giza, Egypt*

³*Faculty of Engineering, Alexandria University, Alexandria, Egypt*

⁴*Department of Computer Engineering, Ahmadu Bello University, Zaria, Nigeria*

Keywords: HMMs, HAR, IMU Sensors, EJUST-ADL-1 Dataset, USC-HAD Dataset, LSTM, RF.

Abstract: Although there are many classification approaches in IMU-based Human Activity Recognition, they are in general not explicitly designed to consider the particular nature of human actions. These actions may be extremely complex and subtle and the performance of such approaches may degrade significantly in such scenarios. However, techniques like Hidden Markov Models (HMMs) have shown promising performance on this task, due to their ability to model the dynamics of such activities. In this work, we propose a novel classification technique for human activity recognition. Our technique involves the use of HMMs to characterize samples and subsequent classification based on the dissimilarity between HMMs generated from unseen samples and previously-generated HMMs from training/template samples. We apply our method to two publicly-available activity recognition datasets and also compare it against an extant approach utilizing feature extraction and another technique utilizing a deep Long Short-Term Memory (LSTM) classifier. Our experimental results indicate that our proposed method outperforms both of these baselines in terms of several standard metrics.

1 INTRODUCTION

Microprocessor and integrated circuit technology have been advanced in leaps and bounds. As such, they have allowed for the production of large numbers of sensors and mobile electronic devices with greater processing capacities and smaller dimensions at extremely low cost. As a result, sensor-driven solutions running on mobile devices for smart homes (Mohammed and Gomaa, 2016), (Mohammed and Gomaa, 2017)), activity tracking, elderly care, and sports evaluations, etc. have come to play a significant role in everyday life. Wearable sensor-based Human Activity Recognition (HAR) is increasingly common for small scale, flexible use and protection of privacy different from any other kind of data acquisition device (Ashry et al., 2018), (Elbasiony and Gomaa, 2019). Nowadays, smartwatches (Ashry et al., 2020), smartphones have multiple accurate sensors to help people better, making them prime candidates for human activity monitoring.

Apps for smartphones and wearable sensors are

capable of differentiating between very distinct physical activities, such as walking and sitting. In addition, previous research could successfully classify complex behaviors such as cooking and washing, which occur by several sensors (Kabir et al., 2016), (Ashry and Gomaa, 2019). However, there is an inherent ambiguity in many day-to-day human actions which are composed of fine movements, which pose recognition problems for activity recognition approaches. To the best of our knowledge, studies are limited in terms of more nuanced discrimination, (e.g. between get up or lie down on bed), with just a few sensors. Such precise activities can be difficult to discern because they require a physical position (stand, sit) and the use of hands to execute or communicate with a particular object. They can also be described as being "detailed" because, compared to other (whole-body) activities, these involve a broader range of simultaneous yet subtle movements. In this vein, several machine learning and biomedical disciplines could benefit from the recognition of detailed activities, including health care, monitoring of the elderly and

lifestyle. This research is therefore focused on the design of a new method for the recognition and monitoring of detailed human activities, using a combination of multiple HMMs and dissimilarity measures. Such research requires the classification of different detailed behaviors. It is our belief that a more accurate view of a subject's health and lifestyle may be provided through more accurate/precise human activity monitoring.

The contributions from this article are as follows:

1) We propose a composite recognition model called multiple HAR-HMM, comprising of individual HMM models per sensor axis per activity. In contrast to previous works, single HMM models are built for each activity to be recognized. Then for a given sample, it calculates the probability of the sample originating from each activity model and chooses the activity with the largest probability as the recognition result.

2) We provide detailed experimental tests and analyses on the performance of the proposed multiple HAR-HMM model. The results suggest that the proposed technique is more reliable in precision, recall, and F-metric compared with the recent study on the same datasets (Gomaa et al., 2017).

The paper is organized as follows. Section 1 introduces the work and its motivations. Section 2 presents a survey of related work. Section 3 presents the methodology of the multiple HAR-HMM model. Section 4 discusses the evaluation of the proposed model. Section 5 concludes the paper.

2 RELATED WORK

2.1 HAR in Literature

In recent years, many studies have addressed the problem of HAR from different perspectives (Abdu-Aguye and Gomaa, 2019), (Abdu-Aguye and Gomaa, 2018), (Abdu-Aguye et al., 2019), (Abdu-Aguye and Gomaa, 2019a), (Abdu-Aguye and Gomaa, 2019b), (Abdu-Aguye et al., 2020a), and (Abdu-Aguye et al., 2020b). The challenge associated with HAR is related to the amount of activities of interest and their characteristics. Lara et al. (Lara and Labrador, 2012) states that the complexity of the pattern recognition problem is determined by the set of activities selected. Also, short tasks, including opening a door or selecting an object, can be done in a wide variety of ways, which increases with the consideration of different users (Kreil et al., 2014).

For physical activity recognition, like walking and standing, a high degree of precision is achieved with smartphones, attributable mostly to the accelerometer (Machado et al., 2015). However, other techniques must be reckoned, for recognizing complicated activities, with similar body movements, such as opening a door and opening a faucet. They considered complex because they almost haven't repetitive patterns like walking, etc. Earlier studies used sound to discriminate activities (Feng et al., 2016). A greater degree of discrimination may be accomplished by incorporating information from many sensors.

Since it is possible to consume the temporal data structure from the Hidden Markov Model (HMM), it became an effective classification technique (Cilla et al., 2009). Some video recognition systems motivated the option of multiple HMMs, one per activity (Gaikwad, 2012); (Karaman et al., 2014). By having one model per activity, some time periods could be ignored in continuous stream analysis. Also, at any moment, new activities could be added to the classification, allowing them to personalize this tool. In addition, temporal sequences, including daily routines, maybe studied without a wide training set.

In summary, several studies have discussed the challenge of human activities from machine vision to ubiquitous sensing. However, there is a lack of prior studies when it comes to short detailed activities. In literature, there is very little evidence of these practices, so this study is an experiment in a poorly explored field of HAR. The classifier chosen is based on many HMMs and the smartwatch is a way to tackle these activities. Its recognition could expand the range of Activities of Daily Living (ADL) and enhance the current HAR systems.

2.2 Used Sensors

The number of sensors and their positions is very important parameters for the design of any sensor-based activity recognition device. In respect of positions of sensors, different parts of the body were selected from feet to shoulders. The locations selected are chosen based on the respective activities. For instance, ambulation activities (such as walking, jumping, running, etc.) were recognized using a waist or a chest sensor (Khan et al., 2010). Whereas, non-ambulation activities (such as combing hair, brushing teeth, eating, etc.) can be classified more effectively using a wrist-worn sensor (Bruno et al., 2013).

The related systems also required obtrusive sensors linked by wired links on the throat, chest, neck, thigh, and ankle. It restricts the freedom of human activity, also obtrusive sensors are not suitable for med-

ical purposes involving elderly or patients with heart disease. In addition, under regulated conditions, some datasets were obtained and a limited number of activities were classified. Such disadvantages are addressed by using a smartwatch on users' wrist and building wide activities in a dataset without oversight under practical conditions as EJUST-ADL-1 dataset collected by our CPS lab.

3 PROPOSED MODEL

3.1 Overview of Proposed Method

In the current work, we represent the framework of this study as shown in Fig 1. we consider all (Inertial Measurement Units) IMU sensors modalities of the smartwatch; especially the accelerometer and gyroscope. This choice is motivated by their ubiquity in virtually all activity recognition datasets, therefore permitting the widespread use of our proposed technique.

For ease of exposition, we describe the proposed technique subsequently using six time-series: three from the triaxial accelerometer and three from the tri-axial gyroscope. When deriving the experimental results (discussed in Section 4.3), we used all the time series available from all the IMU sensors in the chosen dataset(s). However, the proposed technique may be applied in either scenario without a loss of generality.

We begin by denoting some activity as \mathcal{A} . Then, each sample of \mathcal{A} , sam is a six-tuple of timeseries raw data, namely,

$$sam = (a_x, a_y, a_z, g_x, g_y, g_z) \quad (1)$$

where the first three components correspond to the 3 axes of the accelerometer raw data and the last three correspond to the 3 axes of the gyroscope raw data. Each of these components is then used to train a Hidden Markov Model (HMM) that represents the dynamics of the activity in some direction/axis of some sensor modality. Hence, the sample sam is converted to a tuple of HMMs representing that particular sample:

$$H_{sam} = (h_{a_x}, h_{a_y}, h_{a_z}, h_{g_x}, h_{g_y}, h_{g_z}) \quad (2)$$

Subsequently, the HMMs of the samples of activity \mathcal{A} , $\{H_{sam}\}_{sam \in \mathcal{A}}$ are randomly partitioned into two sets. The first set is called $prototypes(\mathcal{A})$, and it is a collection of tuples of HMMs corresponding to a randomly selected subset of the given samples of \mathcal{A} .

These represent templates/prototypes of the activity \mathcal{A} . The complementary set of samples (and their corresponding HMMs) are used for test purposes. For reference, the G-HMMs Training module in Figure 1 is responsible for creating and maintaining the set of prototype HMMs as described.

The exact process of sample classification is described as follows. For reference, these operations are carried out within the G-HMMs Classification module in Figure 1. Given a test sample of 6 timeseries (tri-axial accelerometer and tri-axial gyroscope) $s = (a_x, a_y, a_z, g_x, g_y, g_z)$, we then classify s as belonging to one of the ADL activities using the following procedure:

1. Derive a tuple of HMMs for the given test sample s , each one corresponding to one axis of the sample. Let these models be: $H_s = (h_{a_x}^s, h_{a_y}^s, h_{a_z}^s, h_{g_x}^s, h_{g_y}^s, h_{g_z}^s)$. We describe the particulars of the HMMs in more detail in Section 4.
2. For each activity $\mathcal{A} \in ADL$, and for each prototype sample $s' \in prototype(\mathcal{A})$, do the following:
 - Compute the dissimilarity measure between the HMM tuple H_s and the HMM tuple $H_{s'}$, call it $d(H_s, H_{s'})$. The exact method by which this is done will be discussed subsequently.
3. From the previous step, we obtain a set of dissimilarity scores, one per prototype sample and HMM. Using these scores $\{d(H_s, H_{s'}) : s' \in prototype(\mathcal{A})\}$, calculate one score $D(s, \mathcal{A})$ that indicates the overall dissimilarity of the test sample s to activity \mathcal{A} . We also discuss how $D(s, \mathcal{A})$ is computed below.
4. Using the computed set of dissimilarity scores $\{D(s, \mathcal{A}) : \mathcal{A} \in ADL\}$, identify the most likely activity to generate the test sample s based on the following criterion:

$$\mathcal{A}^* = argmin_{\mathcal{A} \in ADL} D(s, \mathcal{A}) \quad (3)$$

3.2 Inter-sample Dissimilarity

We will now describe the exact manner in which the dissimilarity score between individual samples i.e $d(H_s, H_{s'})$ is computed. Given two HMMs h_1 and h_2 , we use the Kullback-Leibler divergence (KLD) as a base to measure the dissimilarity between the two models (Sahraeian and Yoon, 2011). The *KLD* measures the dissimilarity between two probability density functions as p and q as follows:

$$D_{KL}(p \parallel q) = \int p(x) \log \frac{p(x)}{q(x)} dx \quad (4)$$

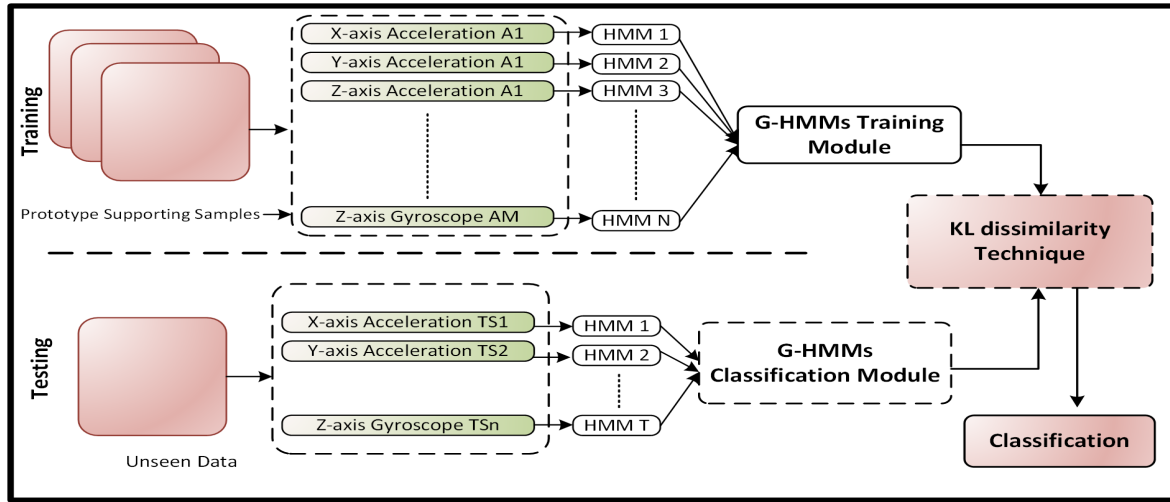


Figure 1: Framework of the proposed model. A^* represents the training/prototype samples across all the considered activities. N is the total number of Hidden Markov Models obtained per-axis across the prototype samples. $TS1 - TSn$ represent the per-axis signals for an unseen sample. T is the number of Hidden Markov Models derived from $TS1-TSn$ which are then compared against the N prototype HMMs to classify the sample.

Typically, no closed-form solution exists for such an integration for probability distributions represented by Hidden Markov Models, so Juang and Rabiner (Juang and Rabiner, 1985) proposed a Monte-Carlo approximation to this integral for comparing two HMMs (Sahraeian and Yoon, 2011) using a sequence of observed symbols. Assume h_1 and h_2 are two HMMs and assume $O = o_1, \dots, o_T$ is an observation sequence of length T , then the KL -dissimilarity between h_1 and h_2 can be approximated by the following formula:

$$D_{KL}(h_1 \parallel h_2) \approx \frac{1}{T} (\log P(O|h_1) - \log P(O|h_2)) \quad (5)$$

In this context the observation sequence O corresponds to some timeseries ts of a sensor in a certain axial direction. As can be seen from (5), KL -divergence is an asymmetric measure. To allow for more natural (i.e commutative) comparison between samples, we derive a symmetric form of the KL -measure as:

$$D_{KL}^{symm} = \frac{D_{KL}(h_1 \parallel h_2) + D_{KL}(h_2 \parallel h_1)}{2} \quad (6)$$

Therefore, given two timeseries ts_1 and ts_2 representing two samples of measurements of some sensor in a particular axial direction (for example, two samples of x -axis of the accelerometer) of two activities (which could be different or the same activity), we compute the dissimilarity score between ts_1 and ts_2 as follows:

1. Let h_1 be the HMM model built from timeseries ts_1 .
2. Let h_2 be the HMM model built from timeseries ts_2 .
3. Compute the log-likelihoods $\log P(ts_1|h_1)$, $\log P(ts_1|h_2)$, $\log P(ts_2|h_1)$, and $\log P(ts_2|h_2)$.
4. Compute the KL -divergence $D_{KL}(h_1 \parallel h_2)$ as follows:

$$D_{KL}(h_1 \parallel h_2) = \frac{1}{|ts_1|} (\log P(ts_1|h_1) - \log P(ts_1|h_2)) \quad (7)$$

where $|ts_1|$ is the length of the timeseries ts .

5. Compute the KL -divergence $D_{KL}(h_2 \parallel h_1)$ as follows:

$$D_{KL}(h_2 \parallel h_1) = \frac{1}{|ts_2|} (\log P(ts_2|h_2) - \log P(ts_2|h_1)) \quad (8)$$

where $|ts_2|$ is the length of the timeseries ts_2 .

6. Compute the symmetric KL -divergence between h_1 and h_2 as in (6).
7. This last quantity represents the dissimilarity score between the timeseries ts_1 and ts_2 .

Given two tuples of timeseries corresponding to sensor measurements $TS = (ts_{ax}, ts_{ay}, ts_{az}, ts_{gx}, ts_{gy}, ts_{gz})$ and $TS' = (ts'_{ax}, ts'_{ay}, ts''_{az}, ts'_{gx}, ts'_{gy}, ts'_{gz})$, we need to compute the dissimilarity measure between these two samples. To do this, we develop the HMM models corresponding to these tuples (12 in total, 6 per sample): $H_{TS} = (h_{ax}, h_{ay}, h_{az}, h_{gx}, h_{gy}, h_{gz})$ and $H_{TS'} =$



Figure 2: Figures showing some activities from the E-JUST-ADL1 dataset (left) and sensor placement from the USC-HAD dataset (right).

$(h'_{ax}, h'_{ay}, h'_{az}, h'_{gx}, h'_{gy}, h'_{gz})$. We use the symmetric KL -divergence ((6)) to find the dissimilarity measure between every pair of corresponding HMMs in the two tuples. Then, these dissimilarity scores along the different axes of the two sensors (accelerometer and gyroscope) are combined together using summation to produce a single dissimilarity score between the two measurement tuples TS and TS' :

$$d(TS, TS') = D_{KL}^{symm}(h_{ax} \parallel h'_{ax}) + D_{KL}^{symm}(h_{ay} \parallel h'_{ay}) + D_{KL}^{symm}(h_{az} \parallel h'_{az}) + D_{KL}^{symm}(h_{gx} \parallel h'_{gx}) + D_{KL}^{symm}(h_{gy} \parallel h'_{gy}) + D_{KL}^{symm}(h_{gz} \parallel h'_{gz}) \quad (9)$$

Then, given two samples s and s' consisting of 6-axial IMU measurements TS and TS' , then the dissimilarity of s and s' is simply taken to be:

$$d(s, s') = d(TS, TS') \quad (10)$$

3.3 Sample-activity Dissimilarity

Given a test sample s corresponding to some unknown activity and a potential activity \mathcal{A} , we compute the dissimilarity between s and \mathcal{A} as follows, considering that we have a set of dissimilarity scores (obtained from the previous section) indicating the dissimilarity between s and each of the prototype samples for \mathcal{A} :

$$d(s, \mathcal{A}) = \min\{d(s, s') : s' \in \text{prototype}(\mathcal{A})\} \quad (11)$$

3.4 Classifying Samples

Adopting the notation from the previous section, we consider that we have computed the sample-activity dissimilarity scores between the unknown sample s and each activity \mathcal{A} in the dataset. Therefore we have as many dissimilarity scores as there are activities in the dataset. Finally, s is assigned to/classified as the activity with the minimum dissimilarity score:

$$\mathcal{A}^* = \text{argmin}_{\mathcal{A}} d(s, \mathcal{A}) \quad (12)$$

4 EXPERIMENTS

In this section we present the details of the experimental procedure used to evaluate our proposed method.

4.1 Datasets Considered

In order to demonstrate the efficacy of our proposed HAR-HMM model, we apply it to two publicly-available activity recognition datasets: EJUST-ADL1 dataset (Gomaa et al., 2017) and USC-HAD (Zhang and Sawchuk, 2012). The details of these datasets are provided in Table 1 and Fig 2.

4.2 Experimental Setup

In order to demonstrate the efficacy of our proposed HAR-HMM model, we perform a number of tests wherein we alter different parameters of the model and investigate their effects on its performance. A total of 4 tests were performed, each test with a different value for the number of hidden states in the HMMs ranging from 2 to 5 states as shown in Table2 .

We also tested the performance of the method in the presence of different sensor combinations as shown in Table 3.

We adopt the following configuration for all tests performed:

- In each test we performed a total of 5 experiments. Results are averaged over those 5 experiments.
- For each activity, the number of samples taken as the prototypes is 66% of the total number of samples. The remaining 34% are used for testing.
- For each experiment we produced the following performance metrics:
 - The confusion matrix for all the 14 activities.
 - The overall accuracy and its 95% confidence interval.
 - The sensitivity and specificity for each activity.
 - The average sensitivity, average specificity, average precision, and average F -score.

We also compare our proposed technique against two other methods: the method presented in (Gomaa et al., 2017) which requires feature extraction, and another involving the use of a deep LSTM-based(Hochreiter and Schmidhuber, 1997) classifier operating directly on the raw data. This is to give a sense of the relative performance of our method juxtaposed against feature extraction-based and other state of the art sequence modelling-based techniques. The deep classifier consisted of a single LSTM layer and

Table 1: Details of Datasets Considered.

Dataset	Number of Subjects	Activities	Sensor Locations	Sensors	Comments
USC-HAD (Zhang and Sawchuk, 2012)	14	Walk forward, walk left, walk right, walk up-stairs, walk down-stairs, run forward, jump, sit on chair, stand, sleep, elevator up, and elevator down	Front right hip	3D accelerometers, 3D gyroscopes	Consists of 12 activities and 2311 samples in total.
EJUST-ADL-1 Dataset (Gomaa et al., 2017)	3	Use telephone, Drink from glass, Pour water, Eat with knife/ fork, Eat with spoon, Climb/ Descend stairs, Walk, Get up/Lie down bed, Stand up/ Sit down chair, Brush teeth, Comb hair	Right wrist only.	3D accelerometers, 3D angular velocity, 3D rotation, 3D gravity.	14 activities are collected using an Apple watch Series 1. Number of samples is 603.

Table 2: Accuracy of method when used with different number of HMM hidden states on E-JUST-ADL1 dataset.

No. of Hidden States	Accuracy
2	91.9%
3	90.95%
4	89.52%
5	82.46%

Table 3: Accuracy of method when used with different sensor combinations on E-JUST-ADL1 dataset.

Combination	Accuracy
Accelerometer	90.9%
Gyroscope	91.62%
Rotation	90.29%
Gravity	91.62%
Accelerometer, Gyroscope, Gravity	90.95%
Accelerometer, Gyroscope, Rotation	87.62%
Acc., Gyro., Rotation, Gravity	91.9%

was trained for 50 epochs with a batch size of 30 samples. We consider accuracy, sensitivity, specificity, precision and F-measure as the metrics of interest. As stated previously, these metrics are aggregated by averaging over each test run.

We use standard definitions for the Precision, Recall, Specificity, F-Measure and Accuracy metrics, described respectively in Equations 13, 14, 15, 16, and 17. We adopt the following notations:

- N is the number of samples in each activity.
- TP refers to the number of true positives.
- FP is the number of false positives.
- TN is the number of true negatives.
- FN is the number of false negatives.

$$Precision = \frac{TP}{TP + FP} \quad (13)$$

$$Sensitivity = \frac{TP}{TP + FN} \quad (14)$$

$$Specificity = \frac{TN}{TN + FP} \quad (15)$$

$$F - Measure = \frac{2 * Precision * Sensitivity}{Precision + Sensitivity} \quad (16)$$

$$Accuracy = \frac{TP}{N} \quad (17)$$

4.3 Discussion

We present the results obtained from our experiments in Table 4. As described previously, we carry out the experiments on two publicly-available datasets. We investigate our proposed technique against a feature extraction-based technique (Gomaa et al., 2017) and a deep classification technique utilizing a Long Short-Term Memory (LSTM) network. Note that these results correspond to a configuration where the HMMs used have only two hidden states each.

As can be observed from the table, our proposed method outperforms both of the comparative techniques used on both datasets in all the considered metrics. Relative to the feature extraction-based method (denoted as RF in the table), our method yields better performance as it (by design) respects the sequential/temporal nature of the data, which is not necessarily guaranteed with many feature extraction-based techniques. Additionally, it can be seen that our method outperforms the deep LSTM-based classifier (denoted as LSTM in the table). This can be attributed to the fact that our method is not only based on sequence-modelling itself, but also includes similarity-based enhancements in contrast to the deep classifier. This allows it to leverage the strengths of both approaches and deliver superior performance to the deep LSTM-based classifier.

Effect of Sensor Choices. We also investigate the performance of the method in the presence of different sensor combinations. This was done with a view to discerning the performance of the method in different scenarios, as activity recognition problems may have different sensor modalities available than the primary evaluations were performed with. We considered single modalities and combinations of modalities as shown in Table 3. For clarity of presentation, we consider only the E-JUST-ADL1 dataset and the accuracy metric in particular.

It can be seen that the method is able to maintain consistent performance even with the use of single

Table 4: A comparison between the proposed HMM-based method, LSTM using raw data, and RF (Gomaa et al., 2017) using two different public datasets.

Dataset	Method	Accuracy	Sensitivity	Specificity	Precision	F-Measure
USC-HAD	RF	78.5%	70.45%	98.2%	60.5%	65.1%
	LSTM	78.57%	72.8%	85.71%	71%	71.88%
	HMM	83.95%	83.8%	98.54%	84.36 %	83.49 %
E-JUST ADL 1	RF	81.64%	82.47%	98.67%	84.6%	83.53%
	LSTM	87.19%	78.5%	93.1%	77%	77.74%
	HMM	91.9%	91.4%	99.37%	92.54%	91.64%

sensors. This is due to its use of both sequence modelling and similarity-based techniques, allowing the system to both capture the intrinsic dynamics of the activity as captured by the sensor(s) used and match samples in that context without explicitly relying on any particular modality. This indicates the reliability of the technique in a multitude of possible deployment scenarios.

Effect of HMM Hidden States. We also experiment with the number of hidden states in the HMMs used. This is done to determine a suitable value for this parameter in the context of the stated task. As stated previously, the initial set of results (Table 4) indicate the performance of the method at 2 hidden states. Therefore we vary the number of hidden states from 3 to 5 for this investigation. Similar to the previous section, we also consider only the E-JUST-ADL1 dataset for clarity and the accuracy metric.

Increasing the number of hidden states in the HMMs has a consistently-increasing detrimental effect on the method. This can be attributed to the fact that the underlying processes generating the time series data per axis are fairly simple, and so increasing the number of hidden states mischaracterizes the process. Therefore, the optimal number of hidden states per HMM in the proposed method is chosen to be 2.

5 CONCLUSION AND FUTURE WORK

In this work, we presented an improved HMM-based technique for human activity recognition based on IMU-sourced data. We evaluate our technique on two publicly-available activity recognition datasets and also compare it against two baseline methods: one based on traditional feature extraction, and the other based on a deep LSTM-based technique using raw data.

The experimental results yielded indicate that the proposed method is effective for the stated task, as it outperforms both baseline methods in terms of several metrics eg., accuracy, sensitivity, specificity, pre-

cision, and F-Measure. A potential drawback of the proposed method is its computational complexity as it requires the training and retention of a large number of HMM models. This weakness can be overcome using parallelization methods such as GPU-based acceleration or similar.

In the future, we intend to investigate the use of multivariate HMMs to cater for single modalities rather than individual HMMs per individual axes' per modality, as well as multivariate HMMs for all the axes simultaneously. Furthermore, we intend to investigate the use of different HMM (dis)similarity measures on the performance of the proposed method.

ACKNOWLEDGMENT

This work is funded by the Information Technology Industry Development Agency (ITIDA), Information Technology Academia Collaboration (ITAC) Program, Egypt – Grant Number (PRP2019.R26.1 - A Robust Wearable Activity Recognition System based on IMU Signals).

REFERENCES

- Abdu-Aguye, M. G. and Gomaa, W. (2018). Novel approaches to activity recognition based on vector autoregression and wavelet transforms. In *2018 17th IEEE International Conference on Machine Learning and Applications (ICMLA)*, pages 951–954. IEEE.
- Abdu-Aguye, M. G. and Gomaa, W. (2019). Competitive feature extraction for activity recognition based on wavelet transforms and adaptive pooling. In *2019 International Joint Conference on Neural Networks (IJCNN)*, pages 1–8.
- Abdu-Aguye, M. G. and Gomaa, W. (2019a). Robust human activity recognition based on deep metric learning. In *n the proceeding of the 16th International Conference on Informatics in Control, Automation and Robotics (ICINCO)*.
- Abdu-Aguye, M. G. and Gomaa, W. (2019b). Versatl: Versatile transfer learning for imu-based activity recognition using convolutional neural networks. In *In the proceeding of the 16th International Conference*

- on *Informatics in Control, Automation and Robotics (ICINCO)*.
- Abdu-Aguye, M. G., Gomaa, W., Makihara, Y., and Yagi, Y. (2019). On the feasibility of on-body roaming models in human activity recognition. In *ICINCO (1)*, pages 680–690. SciTePress.
- Abdu-Aguye, M. G., Gomaa, W., Makihara, Y., and Yagi, Y. (2020a). Adaptive pooling is all you need: An empirical study on hyperparameter-insensitive human action recognition using wearable sensors, accepted. In *IJCNN. The 2020 International Joint Conference on Neural Networks*.
- Abdu-Aguye, M. G., Gomaa, W., Makihara, Y., and Yagi, Y. (2020b). Detecting adversarial attacks in time-series data, accepted. In *ICASSP. IEEE 45th International Conference on Acoustics, Speech, and Signal Processing*.
- Ashry, S., Elbasiony, R., and Gomaa, W. (2018). An LSTM-based Descriptor for Human Activities Recognition using IMU Sensors. In *Proceedings of the 15th International Conference on Informatics in Control, Automation and Robotics - Volume 1: ICINCO*, pages 494–501. INSTICC, SciTePress.
- Ashry, S. and Gomaa, W. (2019). Descriptors for human activity recognition. In *2019 7th International Japan-Africa Conference on Electronics, Communications, and Computations, (JAC-ECC)*, pages 116–119.
- Ashry, S., Ogawa, T., and Gomaa, W. (2020). Charm-deep: Continuous human activity recognition model based on deep neural network using imu sensors of smart-watch. *IEEE Sensors Journal*.
- Bruno, B., Mastrogiovanni, F., Sgorbissa, A., Vernazza, T., and Zaccaria, R. (2013). Analysis of human behavior recognition algorithms based on acceleration data. In *Robotics and Automation (ICRA), 2013 IEEE International Conference on*, pages 1602–1607. IEEE.
- Cilla, R., Patricio, M. A., García, J., Berlanga, A., and Molina, J. M. (2009). Recognizing human activities from sensors using hidden markov models constructed by feature selection techniques. *Algorithms*, 2(1):282–300.
- Elbasiony, R. and Gomaa, W. (2019). A survey on human activity recognition based on temporal signals of portable inertial sensors. In *International Conference on Advanced Machine Learning Technologies and Applications*, pages 734–745. Springer.
- Feng, Y., Chang, C. K., and Chang, H. (2016). An adl recognition system on smart phone. In *International Conference on Smart Homes and Health Telematics*, pages 148–158. Springer.
- Gaikwad, K. (2012). Hmm classifier for human activity recognition. *Computer Science & Engineering*, 2(4):27.
- Gomaa, W., Elbasiony, R., and Ashry, S. (2017). Adl classification based on autocorrelation function of inertial signals. In *Machine Learning and Applications (ICMLA), 2017 16th IEEE International Conference on*, pages 833–837. IEEE.
- Hochreiter, S. and Schmidhuber, J. (1997). Long short-term memory. *Neural computation*, 9(8):1735–1780.
- Juang, B. . and Rabiner, L. R. (1985). A probabilistic distance measure for hidden markov models. *AT T Technical Journal*, 64(2):391–408.
- Kabir, M. H., Hoque, M. R., Thapa, K., and Yang, S.-H. (2016). Two-layer hidden markov model for human activity recognition in home environments. *International Journal of Distributed Sensor Networks*, 12(1):4560365.
- Karaman, S., Benois-Pineau, J., Dovgalecs, V., Mégret, R., Pinquier, J., André-Obrecht, R., Gaëstel, Y., and Dartigues, J.-F. (2014). Hierarchical hidden markov model in detecting activities of daily living in wearable videos for studies of dementia. *Multimedia tools and applications*, 69(3):743–771.
- Khan, A. M., Lee, Y.-K., Lee, S. Y., and Kim, T.-S. (2010). A triaxial accelerometer-based physical-activity recognition via augmented-signal features and a hierarchical recognizer. *IEEE transactions on information technology in biomedicine*, 14(5):1166–1172.
- Kreil, M., Sick, B., and Lukowicz, P. (2014). Dealing with human variability in motion based, wearable activity recognition. In *2014 IEEE International Conference on Pervasive Computing and Communication Workshops (PERCOM WORKSHOPS)*, pages 36–40. IEEE.
- Lara, O. D. and Labrador, M. A. (2012). A survey on human activity recognition using wearable sensors. *IEEE communications surveys & tutorials*, 15(3):1192–1209.
- Machado, I. P., Gomes, A. L., Gamboa, H., Paixão, V., and Costa, R. M. (2015). Human activity data discovery from triaxial accelerometer sensor: Non-supervised learning sensitivity to feature extraction parametrization. *Information Processing & Management*, 51(2):204–214.
- Mohammed, S. A. and Gomaa, W. (2016). Exploration of unknown map for gas searching and picking up objects using khepera mobile robots. In *ICINCO (2)*, pages 294–302.
- Mohammed, S. A. and Gomaa, W. (2017). Exploration of unknown map for safety purposes using wheeled mobile robots. In *ICINCO (2)*, pages 359–367.
- Sahraeian, S. M. E. and Yoon, B. (2011). A novel low-complexity hmm similarity measure. *IEEE Signal Processing Letters*, 18(2):87–90.
- Zhang, M. and Sawchuk, A. A. (2012). Usc-had: a daily activity dataset for ubiquitous activity recognition using wearable sensors. In *Proceedings of the 2012 ACM Conference on Ubiquitous Computing*, pages 1036–1043. ACM.